

The Effect of Gas Ion Bombardment on the Secondary Electron Yield of TiN, TiCN and TiZrV Coatings For Suppressing Collective Electron Effects in Storage Rings

F. Le Pimpec

*Paul Scherrer Institute
5232 Villigen Switzerland*

R.E. Kirby * F.K. King and M. Pivi

*Stanford Linear Accelerator Center,
2575 Sand Hill Road, Menlo Park CA-94025, USA*

Abstract

In many accelerator storage rings running positively charged beams, multipactoring due to secondary electron emission (SEE) in the beam pipe will give rise to an electron cloud which can cause beam blow-up or loss of the circulating beam. A preventative measure that suppresses electron cloud formation is to ensure that the vacuum wall has a low secondary emission yield (SEY). The SEY of thin films of TiN, sputter deposited Non-Evaporable Getters and a novel TiCN alloy were measured under a variety of conditions, including the effect of re-contamination from residual gas.

Key words: Thin film, multipacting, getter, electron cloud, secondary electron emission, ion conditioning

PACS: 79.20.Rf, 79.20.Hx, 81.65.Tx, 29.27.Bd

1 Introduction

The electron cloud effect (ECE) may cause beam instabilities in accelerator structures with intense positively charged bunched beams, and it is expected

* Corresponding author

Email address: `rek@slac.stanford.edu` (R.E. Kirby).

to be an issue for the positron Damping Ring (DR) of the International Linear Collider (ILC). Reduction of the secondary electron yield (SEY) of the beam pipe inner wall is effective in controlling cloud formation. We have previously measured the secondary electron emission (SEE) from a number of technical surfaces and coatings used in ring construction [1], including uncoated aluminium alloys [2]. Here, we present SEY (δ) measurements, after various treatments including ion bombardment, on TiCN, TiN and two differently-deposited non-evaporable getter (NEG) TiZrV films on aluminium substrates. All samples were produced at Lawrence Berkeley National Laboratory (LBNL).

2 Experiment description and methodology

The system used to measure the SEY is described in detail in [2]. Measuring techniques included x-ray photoelectron spectroscopy (XPS) and residual gas analysis (RGA). Sample processing facilities were heating and ion bombardment.

The SEY (δ) definition is determined from equation (1). In practice equation (2) is used because it contains parameters directly measured in the retarding target potential experiment.

$$\delta = \frac{\text{Number of electrons leaving the surface}}{\text{Number of incident electrons}} \quad (1)$$

$$\delta = 1 - \frac{I_T}{I_P} \quad (2)$$

I_P is the primary current (the current leaving the electron gun and impinging on the surface of the sample) and I_T is the total current measured on the sample ($I_T = I_P - I_{SE}$). I_{SE} is the secondary electron current leaving the target.

The SEY is measured, at normal incidence, by using a gun capable of delivering an electron beam of 0-3 keV, working at a set current of 2 nA and having a 0.4 mm² spot size on the target. The measurement of the SEY is done while biasing the sample to -20 V. This retarding field repels most secondaries from adjacent parts of the system that are excited by the elastically reflected primary beam. The primary beam current as a function of the primary beam energy is measured and recorded each time before an SEY measurement, by biasing the target to +150 V, and with the same step in energy for the electron beam. A fresh current lookup table is created with each measurement. The SEY measurement, over the 0-3 keV range, takes around 5 minutes.

In order to study the effect of ion bombardment on the SEY, we used a micro-focussing scanning gas ion gun (Leybold IQE 12/38). The gun has two differentially-pumped beam formation stages that reduce the sample system pressure compared to that inside the gun's electron-impact ionization chamber (into which the gas is directly-injected). Ion energies from 250-5000 eV are possible. Five nines-pure hydrogen or nitrogen gases were used in this particular set of experiments. In an accelerator, the ions produced by beam ionization of residual gases, have a spread in energy. In one of the ILC damping ring designs (6 km), the impact energy of the ions is around 140 eV [3]. Our ion gun is not designed to work below 250 eV; therefore, we have set the energy of the test ions to be 250 eV. The modest increase in ion energy will raise the nitrogen ion (momentum) and hydrogen ion (chemical) sputter yields from 0.1 to 0.15, for removing hydrocarbon contamination [4]. The outermost layers of the aluminium are composed of hydrocarbons and water on top of native oxide. All three materials raise the secondary yield [5]. The nitrogen momentum sputter yield is lower for the native aluminum oxide than for the loosely-bound hydrocarbons and water; however, metal oxides are removable by the hydrogen chemical sputtering [6]. In our setup, the conditioning ions, hydrogen and nitrogen, are impacting onto the sample surface at an angle of 35 ° from the sample normal, with an ion density of $\sim 10^{10} \text{ cm}^{-2}\text{s}^{-1}$. [N.B. This rate is 8 nA on 1" (2.54 cm) diameter sample] The expected species content of the beam, for an electron-impact source using H₂ or N₂, is 50% charged (mostly single-charge diatomic) and 50% charge-exchanged energetic neutrals [7]. However, the beams will be referred to as "H₂⁺" or "N₂⁺".

Table 1
Measurement history of air-exposed thin film samples.

Film	Measured as received	Activated or baked	Vacuum Recontamination	Ion conditioning
TiCN/Al	Y	170°C - 2H	Y	H ₂ 250 eV
NEG A	Y	215°C - 1.75H	Y	N ₂ 250 eV
NEG B	Y	212°C - 2H	Y	-
TiN/Al	Y	-	-	N ₂ 250 eV

The films, deposited on 6063 aluminium alloy substrates, are listed in Table.1, along with their treatment history. The TiZrV NEG films were produced either from an arc-melted cathode (A) or from a sintered powder cathode (B). The two different TiZrV deposition cathodes were used in order to discover which produced dense adherent films of proper stoichiometry. Both did and the results were consistent with the SAES films. The composition in NEG films prepared by CERN and SAES Getters[®] were studied earlier [1]. The composition, in at%, of the coatings TiCN, NEG A&B and TiN is listed in Table.2.

Table 2
Atomic composition (at%) of the different coatings

	Ti	Zr	V	C	N
TiCN	12	-	-	55	33
TiZrV - A	29	25	46	-	-
TiZrV - B	33	25	42	-	-
TiN	51	-	-	-	49

3 Results, TiCN

This ternary film was chosen to be a possible alternative to TiN or NEG coatings. It is known that as-deposited titanium nitride and carbide have a δ_{max} around or below 1 [8,9]; however, after deposition and air exposure, the SEY degrades to such extent that δ_{max} is above 1.5 [1,9,10]. We wanted to test whether a ternary alloy would have different properties when exposed to air than had the pure nitride and carbide. A film was magnetron sputter-deposited from a TiCN cathode in Ar/N₂ atmosphere onto aluminium sheet. The atomic film composition, measured by energy-dispersive x-ray spectrometry, is presented in Table.2. The results are presented in Fig.1.

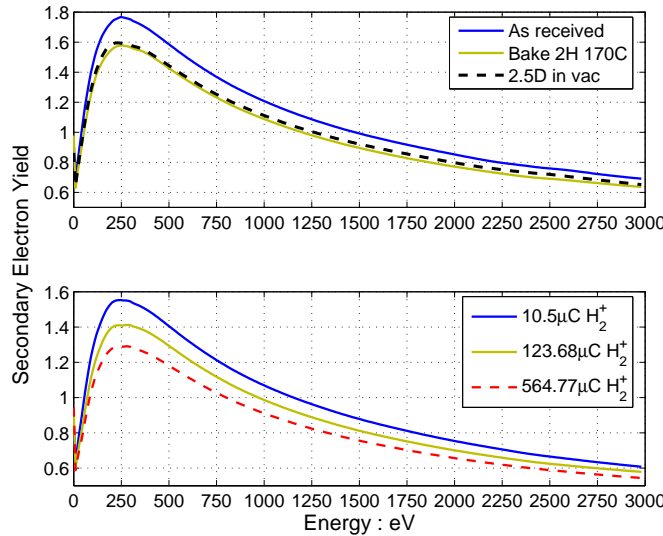


Figure 1. SEY obtained on TiCN/Al sample, at normal incidence, after different accumulated hydrogen ion doses.

The SEY curve and δ_{max} of TiCN, as-deposited and air-exposed ("as-received"), and after heating are similar to that of TiN [11]. Short-term recontamination by residual gas, at a pressure of 5.10^{-10} Torr, had a negligible effect on the SEY.

With respect to ion bombardment behaviour, it is known that a glow discharge (Argon or Nitrogen) (ArGD or NGD) bombardment on technical surfaces will sputter-clean the surface to such an extent that its SEY will be very close from the atomically clean surface [12,13]. We can expect that such plasma will also work on thin films. However, a GD is not sustainable in ultra-high vacuum. That implies a high current of ions impinging the surfaces. It is desirable to reproduce the impact of hydrogen ions, expected to be created by the circulating accelerator beam, on the TiCN coating. Hydrogen, of course, was chosen because it is the highest concentration gas in a baked vacuum environment, Table.3. However, because the ionization cross section is smaller for H_2 than for CO (mass 28), we also tested the effect of using an analog of this much-higher mass projectile on the coatings. CO contaminates vacuum systems with carbon, so equally-massive N_2 was substituted. Chemically-active molecules, like CO, also do adsorption surface chemistry but we expect that this will be a negligible effect compared to the sputtering energy available in the ion beam.

Table 3

System partial pressures, before ion bombardment, at $P_t \sim 2.7 \cdot 10^{-10}$ Torr

Mass (amu)	2	16	28
Current (10^{-10} A)	7	0.2	0.7

During H_2^+ bombardment, the system pressure rose to $1.2 \cdot 10^{-8}$ Torr equivalent N_2 , with 98% of the spectrum dominated by H_2 . Table.4 shows an example of the current recorded by the system RGA during the operation of the ion gun with hydrogen. Taking into account the sensitivity of the ion gauge, the true hydrogen pressure is $2.4 \cdot 10^{-8}$ Torr equivalent H_2 . The effect of the bombardment is shown in Fig.1. Even at this low ion energy and dose, the effect of ion bombardment on the SEY is evident.

Table 4

System partial pressures, during H_2^+ exposure, $P_t \sim 3.6 \cdot 10^{-9}$ Torr

Mass (amu)	2	16	18	28
Current (10^{-9} A)	13.1	0.4	0.1	1.42

XPS-determined surface chemistry showed essentially no changes as a result of ion bombardment (Figure.2). The SEY is significantly more sensitive to surface modification (average escape depth of "true" secondaries ~ 1 nm) than XPS (average escape depth 3-5 nm).

4 Results, TiZrV

The δ_{max} values measured for the "as received" NEG prepared at LBNL, Fig.3, are slightly below the values obtained from the earlier-measured CERN

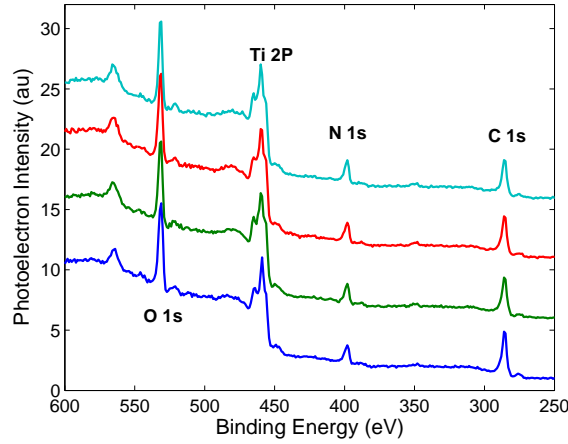


Figure 2. XPS survey spectra of TiCN following different processes. Bottom to top : as received, baked 170° for 2 hours, 2.5 days in vacuum, after $565\mu\text{C}$ of H_2^+ exposure. Spectra are vertically displaced for clarity.

and SAES samples [1], 1.8 versus 1.9 and 2.1, respectively. The SEY values obtained after a 2 hours thermal activation are similar and slightly below 1.2 [1].

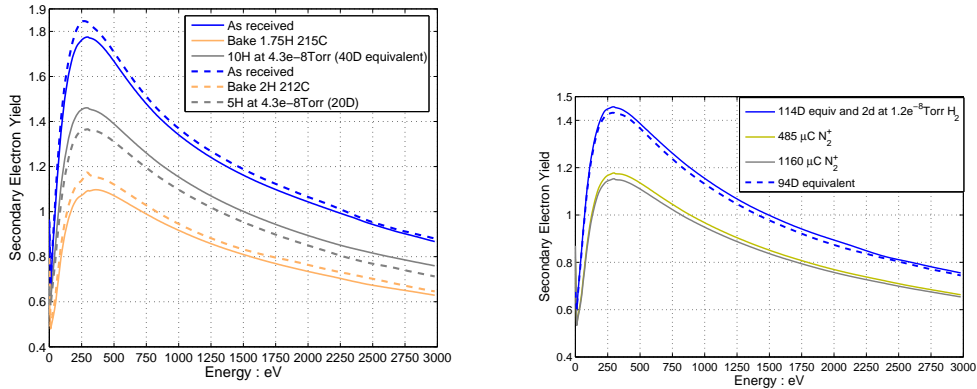


Figure 3. SEY obtained, at normal incidence, on NEG A (Solid line) and NEG B (Dashed line), on both right and left figures. Plots are following the chronology of Table.1.

Residual gas re-contamination of the surface was also studied. The sample was transferred to the higher background pressure of the adjacent load lock chamber. The load lock was unbaked and the total pressure, with the sample, was between 2.10^{-8} Torr and $4.8 10^{-8}$ Torr. This pressure was roughly 100 times above the average pressure in the measurement chamber. The unbaked residual gas composition in the load lock chamber (Table.5) is quite different from that of the measurement chamber, which is dominated by H_2 (Table.3). In reference [1], residual gas exposure was done in the measurement chamber. In this work, it was done in the higher residual pressure of the load lock chamber, to speed up the process. Gas exposure, in this work, is listed in "day

equivalents” of the measurement chamber for easy comparison with the earlier work [1]. Scaling linearly, 1 s spent in the load lock correspond to 100 s spent in the measurement system, for a total pressure in the load lock being 100 times the one in the measurement system. As the saturation is due to sticking of oxygen based molecules, in UHV, and as their sticking factor, on a freshly activated NEG, is at least 10 times the one of hydrogen, comparing directly the total pressure despite being not rigorous is reasonable.

Table 5

Load lock partial pressures, during re-contamination , $P_t \sim 4.6 \cdot 10^{-8}$ Torr

Mass (amu)	2	16	17	18	28	32	44
Current (10^{-12} A)	1.2	0.3	3	10	2.9	0.2	1.5

The SEY max of both NEG samples seems to saturate around 1.42 after 40 days equivalent exposure, dashed line in the left upper plot of Fig.3. For NEG A, there is no difference between the SEY obtained at 40 days equivalent and the one obtained at 114 days equivalent (not shown) as well as the SEY obtained for the NEG being in the load lock for an 114 days equivalent and 2 days inside the measurement chamber during H_2^+ exposure of the TiCN, lower left plot in Fig.3. NEG B show a slight evolution between the 20 days equivalent and 94 days equivalent. However, the SEY max measured is almost equal to the one obtained for NEG A.

With respect to the type of gas molecule that causes the rise in SEY, to saturation (1.42, in our case), Scheuerlein [14] found that CO or water gave the same saturation value (1.4, in his case), and that it is the oxygen-active molecules that matter. The gas adsorption growth rate on the surface is determined by the partial pressure of the gas and by the surface coverage-dependant sticking coefficient of each gas species present. Water vapor is the dominant gas in our load lock and CO in the UHV chamber. Both oxidized the surface to similar condition.

N_2^+ ion-bombardment was performed on NEG A. The δ_{max} decreases and levels off just below 1.2, Fig.3. H_2^+ ion-bombardment was not done on either NEG sample because hydrogen diffusion and embrittlement effects could change the sample morphology [15,16]. Therefore, the NEG was only N_2^+ ion-bombarded.

The NEG A surface chemistry was measured with XPS following the processes listed in Fig.3. XPS analysis from the as-received state (air-exposed getter film) to the activated state has already be discussed elsewhere [1,14,17]. XPS results on re-contamination in vacuum has also been documented with regard to the variation of the SEY [1]. We focus here, instead, on the evolution of the surface under N_2^+ ion bombardment, Fig.4.

After activation, the TiZrV displays C1s carbon peaks at 283 eV and 285 eV binding energy (BE). They are the marks of carbide and of amorphous carbon.

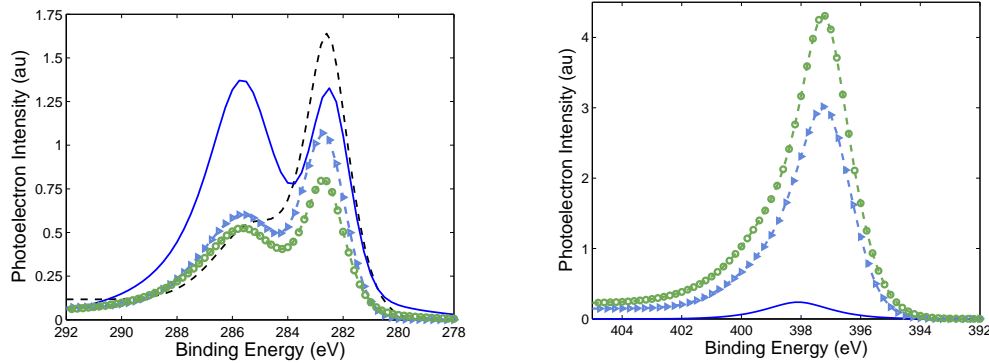


Figure 4. XPS of C1s (left plots) and N1s peaks (right plots) of TiZrV/Al, NEG A, after activation (dashed line), after spending 114 days equivalent in the load lock and after 2 days in an H₂-dominated environment (solid line), exposed to 485 μ C of N₂⁺ ion bombardment (triangles) and exposed to 1160 μ C of N₂⁺ ion bombardment (open circles)

As contamination by the residual gas occurs, mainly by dissociative adsorption of oxygen on the metallic NEG, the 285 eV peak increases and get broadened to higher BE. The broadening is due to contribution of a carbon oxide peak, which sometimes can be well separated from the 285 eV peak. Upon N₂⁺ ion-bombardment, surface molecules/atoms are sputtered away and the carbon and oxygen peak intensities reduce (O 1s data not shown here). Atoms may also be lost from the surface by diffusion, for example, into hot NEG. However, in the latter case, the surface chemistry is not changed significantly, as evidenced by the lack of chemical shifts in the peaks' BE. In other words, the 250 eV N₂⁺ ions do not simply induce bonds re-arrangements. Finally, Fig.4, right plot, shows that nitrogen gets implanted in the NEG and adsorbed. The rather broad spectrum of chemical valence states shows that the nitrogen is populating at least the outer five nm of surface.

The XPS Ti peaks (2p_{1/2} and 2p_{3/2}) do not show changes. However, there was a slight evolution in the Zr3d, Fig.5. Zr has two peaks, located at 178.8 eV and 181.1 eV BE, 3d_{5/2} and 3d_{3/2} respectively. During nitrogen ion bombardment, the intensity of the 3d_{5/2} peak diminishes and the spectrum shifts to slightly higher BE, perhaps indicative of morphology changes.

5 Results, TiN

TiN coating is commonly used to mitigate multipacting in accelerator and storage ring structures [18]. Its SEY properties are rather well known, but not exhaustively so, for a wide range of substrate material, deposition thicknesses and processing conditions [1,9,11,19,20]. This sample was N₂⁺ ion-bombarded (Fig.6), under conditions similar to the TiZrV samples above. The SEY max

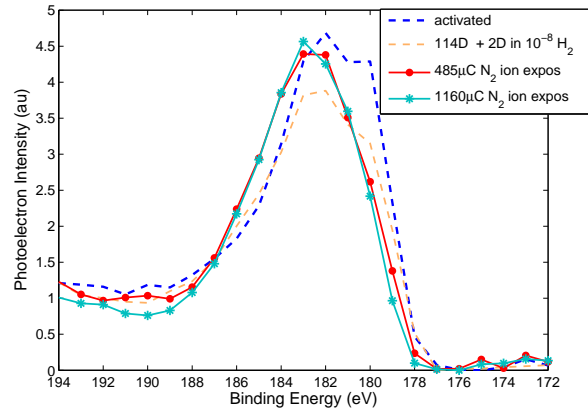


Figure 5. Evolution of the chemistry of Zr 3d

is reduced from 1.5 to 1.1 and is similar to SEY obtained after electron conditioning [1]

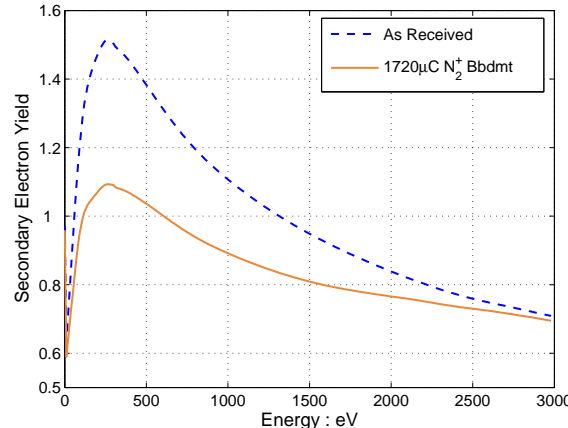


Figure 6. SEY at normal incidence, of coated TiN/Al, as received (dashed line) and after $1720 \mu\text{C N}_2^+$ ion bombardment (solid)

The main peaks of the residual gas present in the measuring system during ion exposure are listed in Table.6. Ar seen in the spectrum could also be released during ion bombardment of the samples. Ar is also used as a medium gas to deposit TiN or NEG films, and is sometimes implanted. However, XPS did not show any traces of Ar in our thin films. The pumping of nitrogen at this level of pressure is sufficient to release noble gas buried in the ion pump cathode plates. Hence, the Ar seen must come solely from the pump.

Table 6

System partial pressures, during N_2^+ bombardment, $P_t \sim 7.10^{-9}$ Torr

Mass (amu)	2	4	12	14	15	16	28	40
Pressure (10^{-11} Torr)	200	3	3	10	1.5	3	100	3

The N_2^+ bombardment removes water, hydrocarbons, and oxygen from oxyni-

tride. Because water and hydrocarbons are a high SEY contaminant, their removal reduces the SEY [5]. The XPS chemistry of the TiN was monitored during bombardment and the main result is presented below, Fig.7. As the surface contamination/oxidation is removed, the Ti 2p and N 1s peak intensities rise. On the contrary, the C 1s and O 1s peaks intensities decrease. The location of all peaks remains unchanged.

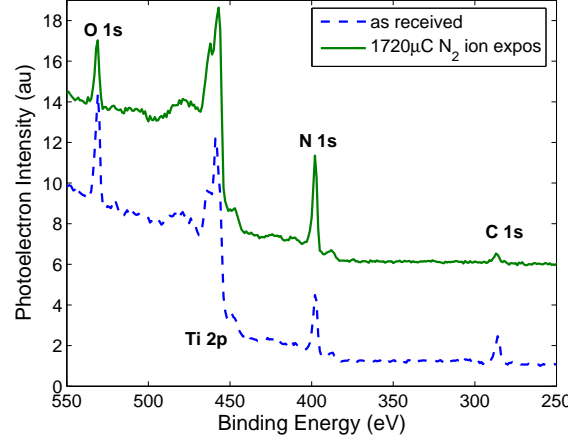


Figure 7. XPS spectra of coated TiN/Al, as received (dashed line) and after $1720 \mu\text{C}$ N_2^+ ion bombardment (solid). Spectra are vertically displaced for clarity.

Ion bombardment by a heavier ion (Ar at 500 eV) could introduce N vacancies [21], and CO_2 gas could play this role. Fortunately, in a baked accelerator, even under the presence of synchrotron radiation, its presence is negligible compared to hydrogen and CO. No extra XPS peaks, for example due to interstitial N, were detected in the spectrum after N_2^+ exposure. This does not mean that vacancies weren't being produced, but they could have been filled by the nitrogen coming from the ion beam.

6 Conclusion

TiCN SEY results, as-received and after heating, do not differ from results obtained on TiN [1]. We expect that, according to the literature, there will also be no advantage in using a simpler TiC coating [9], because it has a similar SEY and behavior upon heating. The important part of this study compares the efficiency of 250 eV ion-bombardment with electron-conditioning. Table.7 shows that a few micro-coulombs per mm^2 of ions is sufficient to bring the SEY max below 1.3. In order to reach such a value with 130 eV electrons, a few thousand times higher dose is needed, Table.8.

It is also not excluded that heavier ions (N_2^+ vs. H_2^+) may be more efficient in conditioning than lighter ions, at least in the case of TiZrV (Fig.3). For a

Table 7
 δ_{max} reduction due to 250 eV ion conditioning

Thin Film	ion species	δ_{max}	Energy _{max}	Dose $\mu C/mm^2$
TiCN	H ₂	1.29	280	1.11
TiN	N ₂	1.09	260	3.39
TiZrV	N ₂	1.15	300	2.29

Table 8
 δ_{max} reduction due to 130 eV electron conditioning. Data obtained at 23 deg from normal incidence [1]

Thin Film	δ_{max}	Energy _{max}	Dose $\mu C/mm^2$
TiZrV/SS(CERN)	1.21	300	11233
TiZrV/Al (SAES)	1.07	370	8425
TiN/Al (LBL)	1.11	290	6829
TiN/Al (BNL)	1.01	380	6529
TiN/SS (BNL)	1.01	290	7720

dose of $0.96 \mu C/mm^2$, the δ_{max} of the TiZrV is already below 1.2. It might also be interesting to now study the effect of CO ion-bombardment vs. CO residual gas adsorption. Based on physical sputtering, conditioning should occur. However, the possibility of surface oxidation by dissociation of the CO could increase the SEY. Exposure to background CO alone does increase the SEY [14]; however, there will be competition for the case of H₂⁺/CO⁺ ion-sputtering vs. CO vacuum recontamination, as is the case for a circulating positron beam.

7 Acknowledgments

This work would not have been carried out without the strong support of Prof T. Raubenheimer and the full ILC team at SLAC. The authors would also like to thank Prof A. Wrulich, at PSI, for his interest in the R&D of the future linear accelerator. This work is supported by the U.S. Department of Energy under contract number DE-AC02-76SF00515.

References

- [1] F. Le Pimpec, F. King, R.E. Kirby, M. Pivi. Properties of TiN and TiZrV Thin Film as a Remedy Against Electron Cloud. *Nuclear Instruments and Methods in Physics Research A*, 551 (2-3):187–199, 2005.
- [2] F. Le Pimpec, F. King, R.E. Kirby, M. Pivi. Electron Conditioning of Technical Aluminium Surfaces: Effect on the Secondary Electron Yield. *Journal of Vacuum Science and Technology*, A (23):1610, 2005.
- [3] L. Wang, SLAC private communication.
- [4] C. Hopf, A. von Keudell and W. Jacob. Chemical sputtering of hydrocarbon films. *J. Appl. Phys.*, 94:2373, 2003.
- [5] J. Halbritter. On Changes of Secondary Emission by Resonant Tunneling via Adsorbates. *Journal de Physique*, 45:C2–315, 1984.
- [6] E. Hoyt, M. Hoyt, R.E. Kirby, C. Perkins, D. Wright and A. Farvid. Processing of OFE copper beam chambers for PEP-II high energy ring. In *PAC95, IEEE Proceedings v.3*, 2075, 1995.
- [7] R.E. Kirby, C.S. McKee and L.V. Renny. Faceting of Cu(210) and Ni(210) by activated nitrogen. *Surface Sci.*, 97:457, 1980.
- [8] David R. Lide, editor. *Handbook of Chemistry and Physics*. 74th edition. CRC PRESS, 1994.
- [9] E.L Garwin F.K. King R.E. Kirby and O. Aita. Surface Properties of Metal-Nitride and Metal-Carbide films deposited on Nb for radio-frequency superconductivity. *Journal of Applied Physics*, 61(3), 1987.
- [10] P. He et al. Secondary Electron Emission Measurements for TIN coatings on the Stainless Steel of SNS Accumulator Ring Vacuum Chamber. In *EPAC 2004*, 2004. SLAC-PUB-10570.
- [11] N. Hilleret, 2002. <http://laser.jlab.org/devlore/filebin/6701/HPC2002/talks/hilleret.pdf>.
- [12] R. Calder, G. Dominichini, N. Hilleret. Influence of various vacuum surface treatments on the secondary electron yield of Niobium. *Nuclear Instruments and Methods in Physics Research B*, B13:631, 1986.
- [13] H. Padamsee and A. Joshi. Secondary electron emission measurements on materials used for superconducting microwave cavities. *Journal of Applied Physics*, 50(2):1112, 1979.
- [14] C. Scheuerlein. The Activation of Non-evaporable Getters Monitored by AES, XPS, SSIMS and Secondary Electron Yield Measurements. Technical report, 2002. CERN- THESIS- 2002- 026.
- [15] P. Chiggiato, CERN private communication.

- [16] Y. Li, Cornell University private communication.
- [17] M. P. Lozano and J. Fraxedas. XPS Analysis of the Activation Process in Non-Evaporable Getter Thin Films. *Surface and Interface Analysis*, 30:623, 2000.
- [18] K.M. Welch. Low Pressure Crossed Field Vacuum Sputtering of Thin Films for Multipactor Suppression Using a Simple Diode Array. Technical report, SLAC-Pub-1472, 1974.
- [19] R.E. Kirby, F.K. King. Secondary Emission Yield from PEP-II accelerator material. *Nuclear Instruments and Methods in Physics Research A*, A469, 2001.
- [20] L. Galán, et al. Surface Treatment and Coating for the Reduction of Multipactor and Passive Intermodulation (PIM) Effects in RF Components. In *4th International Workshop on Multipactor, Corona and PIM in Space Hardware*, 2003.
- [21] P. Prieto and R.E. Kirby. X-ray photoelectron spectroscopy study of the difference between reactively evaporated and direct sputter-deposited TiN films and their oxidation properties. *Journal of Vacuum Science and Technology*, A13(6), 1995.

List of Tables

1	Measurement history of air-exposed thin film samples.	3
2	Atomic composition (at%) of the different coatings	4
3	System partial pressures, before ion bombardment, at $P_t \sim 2.7 \cdot 10^{-10}$ Torr	5
4	System partial pressures, during H_2^+ exposure, $P_t \sim 3.6 \cdot 10^{-9}$ Torr	5
5	Load lock partial pressures, during re-contamination , $P_t \sim 4.6 \cdot 10^{-8}$ Torr	7
6	System partial pressures, during N_2^+ bombardment, $P_t \sim 7 \cdot 10^{-9}$ Torr	9
7	δ_{max} reduction due to 250 eV ion conditioning	11
8	δ_{max} reduction due to 130 eV electron conditioning. Data obtained at 23 deg from normal inc	

List of Figures

1	SEY obtained on TiCN/Al sample, at normal incidence, after different accumulated hydrogen doses	
2	XPS survey spectra of TiCN following different processes. Bottom to top : as received, baked	
3	SEY obtained, at normal incidence, on NEG A (Solid line) and NEG B (Dashed line), on both TiCN/Al samples	
4	XPS of C1s (left plots) and N1s peaks (right plots) of TiZrV/Al, NEG A, after activation (dashed line) and as received (solid line)	
5	Evolution of the chemistry of Zr 3d	9
6	SEY at normal incidence, of coated TiN/Al, as received (dashed line) and after 1720 $\mu\text{C N}_2^+$	
7	XPS spectra of coated TiN/Al, as received (dashed line) and after 1720 $\mu\text{C N}_2^+$ ion bombardment	